PERGAMON

International Journal of Heat and Mass Transfer 44 (2001) 4345–4357

International Journal of HEAT and MASS TRANSFER

www.elsevier.com/locate/ijhmt

Heat transfer enhancement by the chimney effect in a vertical isoflux channel

A. Auletta [a], O. Manca [a], B. Morrone [a], V. Naso [b,*]

[a] *Dipartimento di Ingegneria Aerospaziale, Seconda Università degli studi di Napoli Real Casa dell'Annunziata, Via Roma 29-81031, Aversa (CE), Italy*

[b] *Dipartimento di Energetica, Termofluidodinamica applicata e Condizionamenti ambientali Università degli studi Federico II, Piazzale Tecchio 80125, Naples, Italy*

Received 4 February 2000; received in revised form 24 November 2000

Abstract

The ease of thermal control by means of air natural convection stimulates the investigation of configurations with the aim at improving the thermal performance. The effect of adding adiabatic extensions downstream of a vertical isoflux symmetrically heated channel has been experimentally analyzed. Optimal configurations have been identified through the measured wall temperature profiles, with reference to the extension and expansion ratios (L/L_h and B/b) of the insulated extensions. Conspicuous maximum wall temperature reductions have been achieved by means of these optimal configurations. In details, percent increases of the heat transfer rate (i.e., average channel Nusselt number) were of order 10–20% depending on the channel aspect ratio, L_h/b, and imposed wall heat flux. In any case, quite large extensions should be added to enhance the heat transfer rate, i.e. about 3.0 times the height of the channel, while the optimal expansion ratio was nearly 2.0 for all the configurations. Composite correlations between the average Nusselt number and the maximum dimensionless wall temperatures and Ra^*, the Rayleigh channel number, B/b and L/L_h parameters, in the $1.5 \leqslant L/L_h \leqslant 4.0, 1.0 \leqslant B/b \leqslant 4.0$ and $10^2 \leqslant Ra^* B/b \leqslant 5.0 \times 10^6$ ranges, have been evaluated. © 2001 Elsevier Science Ltd. All rights reserved.

1. Introduction

Nowadays more recent investigation trends in natural convective heat transfer are oriented towards either the seeking of new configurations to enhance the heat transfer parameters or the optimization of standard configurations. This is true in particular for thermal design in cooling of electronics as it has been well explained in [1–3] recently. In fact, the continuously growing heat transfer rates to be dissipated force researchers to focus their efforts to improve the heat transfer coefficients, without renouncing the cheap and reliable natural convection mechanism.

A configuration where natural convection heat transfer has been widely studied is the heated vertical parallel plates, as reported in [4–6] and reviewed more recently in [7]. This review does not need to be repeated here. Several authors tried to optimize the thermo-geometrical configurations to enhance the heat transfer, both from the experimental side and from the numerical one, as for example in [2,3,8].

One of the techniques employed to improve the heat transfer rate is the placement of adiabatic extensions downstream of the heated channel. This induces an increment of the flow rate due to the well-known chimney effect. Haaland and Sparrow [9] were the first researchers who showed that a higher flow rate of fluid through a confined open-ended enclosure can be induced by the chimney effect. They accomplished a numerical solution for natural convection flow in a vertical channel with a point heat source (channel plume problem) or distributed heat sources situated at the channel inlet (chimney problem). Oosthuizen [10] numerically studied the heat transfer enhancement caused by the addition of straight adiabatic extensions at the exit of isothermal

* Corresponding author. Tel.: +39-081-768-2302; fax: +39-081-239-0364.

E-mail address: vinaso@unina.it (V. Naso).

0017-9310/01/$ - see front matter © 2001 Elsevier Science Ltd. All rights reserved.
PII: S0017-9310(01)00064-3

Nomenclature

b	channel spacing, m
B	extension spacing, m
g	acceleration of gravity, m s^{-2}
Gr	Grashof number, Eq. (2)
k	thermal conductivity, W m^{-1} K^{-1}
L	total length, $L_{ext} + L_h$, m
L_{ext}	extension length, m
L_h	channel length, m
Nu	average channel Nusselt number, Eq. (4)
Pr	Prandtl number
q	heat flux, W m^{-2}
r	regression coefficient
Ra^*	channel Rayleigh number, Eq. (2)
T	temperature, °C
T^*	dimensionless temperature, Eq. (6)
x, y, z	coordinates, m
X	dimensionless x coordinate, Eq. (1)

Greek symbols

β	volumetric coefficient of expansion, K^{-1}
v	kinematic viscosity, m^2 s^{-1}

Subscripts

c	convective
k	conductive
max	maximum
o	ambient air
r	radiative
w	wall
Ω	ohmic dissipation

parallel-walled channel. He solved the parabolic form of the governing equations by means of a fully implicit forward marching procedure. The results indicated that substantial increases (about 50%) in the heat transfer rates could be achieved but that very long adiabatic sections were required. Wirtz and Haag [11] obtained experimental results for isothermal symmetrically heated plates with an unheated entry channel portion. Their investigation was carried out over a wide range of the Rayleigh number, from the single-plate limit to the fully developed channel. They found that the flow is quite insensitive to the presence of the unheated entry section for large channel spacings, while it is severely affected when the gap spacing is small. Asako et al. [12] examined numerically the heat transfer increment due to an unheated chimney attached to a vertical isothermal tube. The numerical results were obtained by a control volume approach solving the full elliptic form of the governing equations. They evaluated the optimum chimney diameter where the maximum amount of heat is transferred and found that for optimum chimney diameters the heat transfer enhancement was up to 2.5 times for low Rayleigh numbers and small chimney sizes. Straatman et al. [13] carried out a numerical and experimental investigation of free convection in vertical isothermal parallel-walled channels, with adiabatic extensions of various sizes and shapes. They employed a finite element discretization to solve the fully elliptic form of the governing equations with the inlet boundary conditions based on Jeffrey–Hamel flow. The experiments were performed with ambient air, using a Mach–Zender interferometer. The increase in heat transfer rates varied from 2.5 times at low Rayleigh numbers to 1.5 times at high Rayleigh numbers. The authors proposed a single correlation in terms of the channel Rayleigh number and all the geometric parameters (heated length ratio, expansion ratio). Lee [14] investigated numerically the effects of the unheated entry or unheated exit section on natural convection in vertical channels with isotherm or isoflux walls. The results were obtained by means of the boundary layer approximation and an important finding was that an unheated exit determines larger total heat transfer and flow rate than an unheated entry does. Campo et al. [7] presented numerical solutions to the wall temperature distribution and the thermal and fluid-dynamic fields in a channel with partially isoflux heated parallel plates. They found a reduction in the maximum wall temperature when an insulated extension was placed downstream of the heated part, the larger the Rayleigh number the less relevant the reduction. Fisher et al. [15] and Fisher and Torrance [16] developed analytical solutions for a vertical parallel plate isothermal heat sink and chimney system [15] and for a pin-fin sink and chimney system [16]. In the former investigation a ridge of maximum total heat transfer was observed with respect to the plate spacing and the heat sink height, and the authors showed that smaller heat sinks can be used together with a chimney without compromising the thermal performance and without increasing the system size. In the latter, the chimney effect was shown to enhance local heat transfer rates in such a way that the minimum temperature rise remains approximately constant while the height of the heat sink relative to the total height is reduced. Bianco et al. [17] studied experimentally the same geometrical configuration presented in [13] but with the heated part at uniform wall heat flux. They presented a limited investigation in terms of geometric parameters and Rayleigh numbers. Shahin and Floryan [18] analyzed numerically the chimney effect in a system of isothermal multiple vertical channels (periodic channel expanded chimney). Each channel had an adiabatic extension, just like the geometry studied in [13]. They claimed that the interaction between multiple channels increases the induced flow rate and that the

associated chimney effect is stronger than in a single channel with adiabatic extensions. Fisher and Torrance [19] carried out experiments on air natural convection in a finned vertical parallel plate heater, with an adiabatic downstream extension. The effect of the fin spacing and the channel length on the total heat transfer was investigated and results confirmed prior theoretical predictions.

It is worth noting that, apart from the studies in [11,13,19], the chimney effect in channels has not been deeply investigated from the experimental point of view, particularly with uniform heat flux at walls. In addition, as pointed out by Asako et al. [12], the optimal thermal configurations can be sought by considering the physics of the problem. In fact, the addition of insulated extensions downstream of the heated part brings an increment of the induced mass flow rate. By fixing the extension height, an optimal gap should exist between the two limiting cases, i.e. when there are no extensions (no augmentation at all) and when this gap tends to infinity.

In this paper an experimental investigation, focused on the seeking of optimal configurations, is presented. Wall temperature profiles along the channel length and maximum wall temperatures are reported. The optimal configurations are obtained in terms of the minimum values of maximum wall temperatures. Average Nusselt numbers have been evaluated and presented in the 10^{-1}–10^{6} range of the Rayleigh number. Furthermore, useful correlations are suggested which allow the thermal electronic designers to choose the best thermal configuration.

2. Experimental apparatus

The investigated test section is shown in Fig. 1, where x, y and z are the axial coordinate, the coordinate along the channel gap and the coordinate orthogonal to the picture plane, respectively. The configuration (Fig. 1(a)) was made of two symmetrically heated vertical parallel plates (*channel*) and a downstream unheated region (*chimney*). The channel was made of two heated plates,

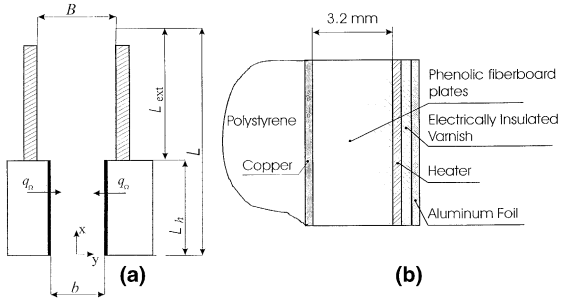

Fig. 1. Sketch of the test section.

each of them was a 3.2-mm thick and 530-mm wide phenolic fiberboard plate, with a typical thermal conductivity of 0.17 W m^{-1} K^{-1}. Their surface facing the channel was coated with a 16-μm thick copper layer, which was the heater. Heat losses from the back of each wall of the channel were reduced by sticking a 120 mm polystyrene block on the rear surface of each wall. The cross-section of the heated wall is reported in Fig. 1(b). Each heater was obtained by cutting the copper in a 4.6-mm wide and 9.0-m long serpentine track. Its expected electric resistance was about 0.50 Ω. A thick copper bar, bolted to the electric supply wire, was soldered to the ends of each heater. No electric resistance between the heater and the bars was measured during preliminary tests. A direct electrical current was passed through the copper and the dissipated heat rate was evaluated with an accuracy of ±2%, by measuring the voltage drop and the current through the electric resistance. A maximum variation of ±10% in the electrical resistivity of the copper was evaluated in the worst conditions, when the maximum difference in the wall temperatures was 30 K. Therefore, a uniform wall heat flux was assumed, with a ±5% maximum deviation from its average value.The typical time interval to attain steady-state conditions after modifying the electric power supply was nearly 3 h. The chimney was made out of two 30-mm thick and 530-mm wide polystyrene blocks. The total normal emissivity of the heated and unheated walls was 0.1. It was obtained by sticking a self-adhesive 25-μm thick aluminum foil on the surfaces facing the channel. The emissivity was evaluated by means of radiometric direct measurements. The electric insulation between the copper surfaces and the aluminum foil was assured by uniformly spraying an electrically insulating varnish onto them before coating. Side walls of the channel and of the chimney were made of Plexiglas rectangular rods placed between the walls at their lateral edges. The rods were machined within an accuracy of ±0.03 mm. A caliper measured the gap of the channel with an accuracy of ±0.025 mm and the gap of the insulated extensions with an accuracy of ±0.50 mm. The channel was open to the ambient only along the top and the bottom edges. The walls were fastened together by a steel frame, which was designed in such a way as not to obstruct the fluid flow in the proximity of the channel inlet. The channel and the chimney were aligned vertically, with horizontal leading edges, by means of a plumb line and a level. The clearance of the bottom edges of the heated walls above the floor was 1.20 m and the minimum distance between the exit section of the chimney and the ceiling was 1.80 m. The entire apparatus was located in an enclosed room, accurately sealed in order to eliminate extraneous air currents and air drafts were further reduced by vertical screens, 2.5 m high. A large fraction of the lower part of the screens was made up by a 0.20-m high mesh. The measured differences in the air ambient

temperature in the proximity of the inlet and the exit sections of the apparatus were less than 0.8 K.

The channel and the chimney were 475 mm wide. The length of the channel was $L_h = 100$ mm and that of the chimney, L_{ext}, varied in the 0–300 mm range. The channel spacing, b, varied in the 10–40 mm range; that of the chimney, B, varied in the 10–200 mm range. With these dimensions, the channel aspect ratio L_h/b was in the 2.5–20 range and the expansion ratio B/b ranged between 1.0 and 8.0.

Wall temperature measurements were carried out by 0.50 mm OD copper–constantan (type T) thermocouples, embedded in the fiberboard in the very proximity of the back side of the copper layer and bonded with a 3 M epoxy glue. They were run horizontally, parallel to the surfaces, thereby lying along isotherms in order to minimize conduction heat losses in the leads. Ten equally spaced thermocouples were placed in the centerline of each plate: the first was placed 5.0 mm downstream of the inlet section, the distance between two successive thermocouples being 10 mm. At 75 mm from the leading edge of one of the heated walls, eight additional thermocouples were located horizontally outward from the centerline at $z = \pm 75.0$, ± 100.0, ± 125.0 and ± 150.0 mm, in order to provide indications of the horizontal variation of the wall temperature. The ambient air temperature was measured by the same type of thermocouples located in the proximity of the leading edge of the channel. Fifteen thermocouples were affixed to the rear surface of the plates and embedded in the polystyrene block, in order to evaluate the conductive heat losses. Thermocouple voltages were recorded to 1 μV. Each thermocouple was calibrated in a 0.01 K thermostatic bath by means of a reference standard thermometer (Pt 100). The calibration of the temperature measuring system showed an estimated precision of the thermocouple-readout system of ±0.1 K. A National Instruments SCXI module data acquisition system and a personal computer were used for the data collection and reduction. The data acquisition was performed through the LabView™ software.

Tests showed the wall temperature to be symmetric in the two heated plates at the same x location, the differences being within ±0.2°C. Wall temperature was assumed to be independent of z coordinate within $z = \pm 100$ mm, since in this region its maximum deviation from the centerline temperature was found to be no larger than 1.0°C when the latter was 70.0°C. No fluctuations in the wall temperature were measured during the tests.

3. Data reduction

The dimensionless coordinate along the length is

$$X = \frac{x}{L_h}. \tag{1}$$

The channel Rayleigh number is defined as

$$Ra^* = Gr\frac{b}{L_h}Pr = \frac{g\beta q_c b^4}{\nu^2 k}\frac{b}{L_h}Pr, \tag{2}$$

where q_c is the mean value of the spatially averaged convective heat flux

$$q_c = \frac{1}{L_h}\int_0^{L_h} q_c(x)\,dx. \tag{3}$$

The channel Nusselt number is based on the difference between the wall and the inlet fluid temperatures, rather than on that between the wall and the bulk fluid temperatures, since the last one cannot be easily measured in practical applications:

$$Nu = \frac{q_c b}{(T_w - T_o)k} \tag{4}$$

with the average wall temperature defined as

$$T_w = \frac{1}{L_h}\int_0^{L_h} T_w(x)\,dx. \tag{5}$$

The dimensionless wall temperature is

$$T_w^* = \frac{(T_w - T_o)k}{q_c b}. \tag{6}$$

The properties of the air are evaluated at the reference temperature $(T_w + T_o)/2$.

Local convective heat flux, $q_c(x)$, is not uniform because of radiation and conduction. Experimental data are reduced by first introducing, in the equations presented above, the local convective heat flux

$$q_c(x) = q_\Omega(x) - q_k(x) - q_r(x). \tag{7}$$

In Eq. (7) the overall heat rate divided by the area of the heated wall surface is the local heat flux due to ohmic dissipation, $q_\Omega(x)$, which was assumed to be uniform along the heated plates; $q_k(x)$ denotes the local conduction heat losses from the plates and $q_r(x)$ is the local radiative heat flux from the plates. For each run, the terms $q_k(x)$ were calculated by a finite difference numerical procedure, a two-dimensional distribution of the temperature being assumed in the polystyrene. The predicted temperatures in significant configurations of the system had been previously compared to those measured by the thermocouples embedded in the polystyrene insulation and the agreement was very good, the maximum deviation being 4%. The $q_r(x)$ terms were calculated for each temperature distribution in the walls, ambient temperature and channel spacing, dividing each plate into 10 equal length strips along the channel, according to the procedure described by Webb and Hill [20]. For all the investigated configurations the conductive heat losses were about 9% of the ohmic wall heat flux, whereas the radiative ones ranged between about 3% and 5%.

Table 1
Maximum percent uncertainty values ($(\delta X_i/X_i)\times 100$)

Variable	T_w	T_o	$T_w - T_o$	b	q_c	q_r	q_Ω	q_k
Uncertainty	0.50	0.93	1.1	1.2	3.0	5.0	2.0	4.0

4. Uncertainty analysis

The uncertainty in the calculated quantities was determined according to the standard single sample analysis recommended in [21,22]. Accordingly, the uncertainty of a dependent variable R as a function of the uncertainties in the independent variables X_i is given by the relation

$$\delta R = \left[\left(\frac{\partial R}{\partial X_1}\delta X_1\right)^2 + \left(\frac{\partial R}{\partial X_2}\delta X_2\right)^2 + \cdots + \left(\frac{\partial R}{\partial X_n}\delta X_n\right)^2\right]^{1/2}. \tag{8}$$

The uncertainty in the values of the air thermophysical properties can be assumed to be negligible. On the basis of Eqs. (2), (4), (6) and (7) and of the maximum percent uncertainties in the values of the independent variables, which are reported in Table 1, the maximum uncertainty in Ra^* ranged from 5–8% whereas the maximum uncertainty in Nu turned out to be 4–7%.

5. Results and discussion

Since one of the main aims of the present paper is to cope with the sensitivity analysis of the heat transfer parameters as a function of the thermal and geometrical parameters, which characterize the system, rather large ranges of the latter have been investigated. With this in mind and with reference to Fig. 1, the wall temperature profiles for $L_h/b = 2.5, 5.0$ and 10, $q_\Omega = 100, 300$ and 450 W m^{-2}, $L/L_h = 1.0, 1.5, 2.0, 3.0$ and 4.0 and B/b ranging between 1.0 and 8.0 are reported in the following. The configuration with $L/L_h = 1.0$ is the simple channel without insulated extensions, which in the following will be referred to as *base case*. It should be taken in mind that the configuration with $B/b \to \infty$ physically coincides with the base case ($L/L_h = 1.0$).

5.1. Wall temperature profiles

The wall temperature profiles along the axial coordinate, in the heated part of the system, at different expansion ratio values, B/b, are reported in Fig. 2, with an aspect ratio $L_h/b = 10$, dissipated heat fluxes of 100 and 300 W m^{-2} and an extension ratio, L/L_h, equal to 1.5 and 3.0. When L/L_h is equal to 1.5, Fig. 2(a), and the expansion ratio is equal to 1.0 the wall temperatures are greater than those for $B/b \to \infty$, i.e. without extensions (base case). As already noticed in [20,23], we can remark that in the base case the temperature profile exhibits a dip in the proximity of the exit section of the channel. These edge effects are due to the convective and radiative heat transfer to the ambient, which are stronger in the upper region of the channel. The dip in the wall temperature is less pronounced when the chimney walls are aligned with the channel walls ($B/b = 1$) since in this case the convective heat transfer to the ambient vanishes. On the contrary, in all cases with $B/b > 1$, the larger B/b the larger the wall temperature decrease. As B/b increases, the wall temperatures show lower values than for the base case and, in addition, a minimum is found at $B/b = 2.0$. The reduction of wall temperatures for B/b values larger than 1.0 depends on two causes. The first is the enhanced chimney effect due to the insulated extension, which implies an increase in the *effective height* of the channel and a subsequent increment in the buoyancy force. The second is the following: for a fixed length of the adiabatic extensions, an increment of their spacing determines a pressure recovery in the unheated region and a low-pressure zone at the exit of the channel. Both these effects concur to enhance the chimney effect. As it was already observed in this figure, when $L/L_h = 1.5$ and the expansion ratio B/b is 2.0, a noticeable optimum is found in terms of wall temperatures. The greater the B/b, the greater the wall temperatures, since the adiabatic extensions are not long enough to act as a shroud with respect to the flow coming from the chimney. In fact, an inflow of cold air from the outer ambient cools the thermal plume exiting the channel, implying a weaker chimney effect. As it can be seen in Fig. 2(b), which refers to the configuration with $L/L_h = 3.0$, the thermal performance of the channel is considerably better than the base case at any B/b and $B/b = 4.0$ yields the best thermal performance for this value of L/L_h. In contrast, when $B/b = 8.0$ the system behaves the same way as for $B/b = 1.0$. A similar behavior is observed at the larger heat flux value ($q_\Omega = 300$ W m^{-2}), Figs. 2(c) and (d). When $L/L_h = 1.5$ (Fig. 2(c)) the wall temperature profiles lay in a very narrow band, except for the case with $B/b = 2.0$. Even when $L/L_h = 3.0$ (Fig. 2(d)), almost all the configurations show nearly the same pattern of wall temperature profiles. The configuration with $B/b = 4.0$ is very close to the optimal one, which is attained at $B/b = 2.0$. Finally, comparing Figs. 2(a)–(d), one can notice that a longer chimney determines a better thermal performance, whichever the B/b ratio.

The temperature profiles, for the configurations with $L_h/b = 5.0$, the extension ratio L/L_h equal to 1.5 and 3.0,

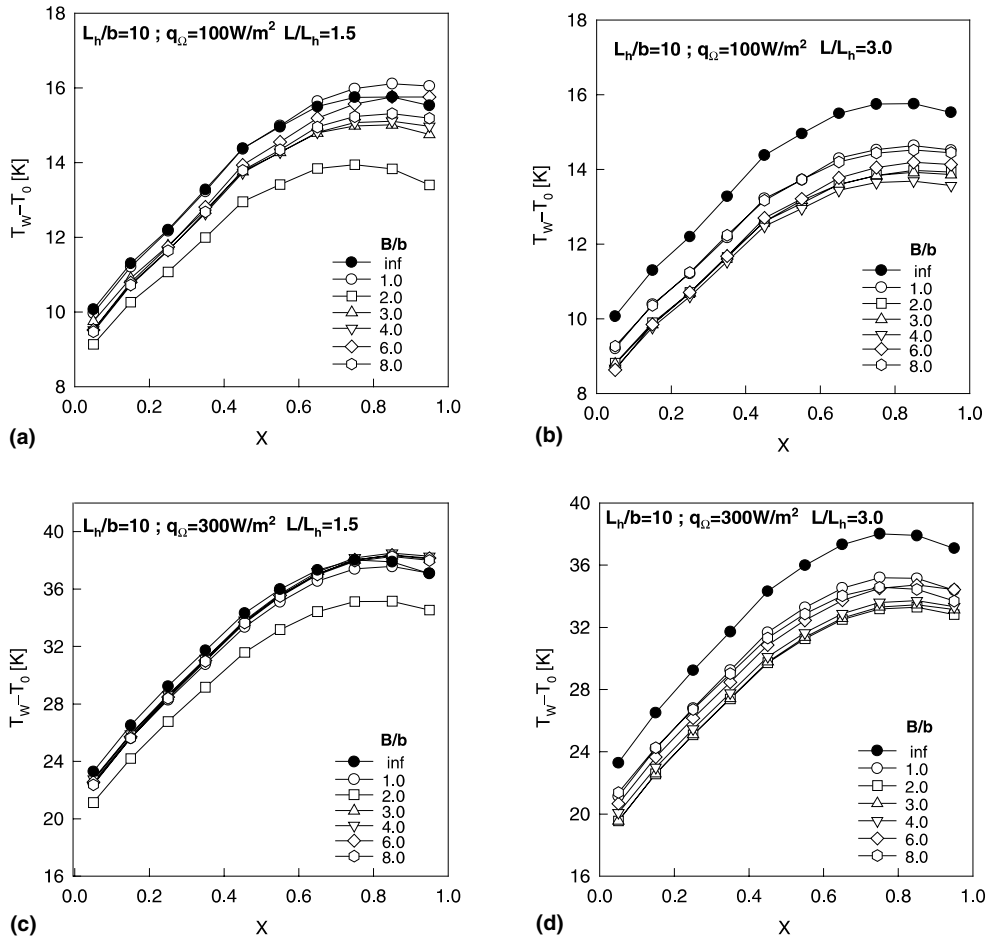

Fig. 2. Wall temperature profiles with $L_h/b = 10$ for several expansion and extension ratio values and two ohmic wall heat fluxes.

at different values of the expansion ratio B/b and several dissipated heat fluxes (300 and 450 W m^{-2}) are reported in Fig. 3. All the configurations show a stronger decrease in the wall temperatures close to exit section since the edge effects are larger than the previous case. Almost all the tested configurations show a better thermal performance than the base case, even if the shrouding effect of the insulated extensions vanishes as B/b increases. The configurations at $B/b = 2.0$ and 3.0 show nearly the same thermal performance. At $q_\Omega = 300$ W m^{-2} (Figs. 3(a) and (b)), the wall temperature profiles in the channel attain slightly lower values when $B/b = 1.0$ than the base case. On the other hand, at the channel exit the temperature differences are larger. This occurs because the edge effects are more evident without the adiabatic extensions, since the trailing edge of the plate can directly transfer heat to the ambient, as it was already observed. The larger the expansion ratio the better the heat transfer performance, up to an optimal value for each configuration (i.e., for fixed $q_\Omega, L_h/b$, L/L_h); then it worsens at increasing B/b values. The sensitivity analysis of the B/b parameter shows that the base case ($B/b \to \infty$) performs in an intermediate way when $L/L_h = 1.5$, while it performs worse for the larger L/L_h value. At $q_\Omega = 450$ W m^{-2} the adiabatic extensions always imply at any B/b, a better thermal performance than in the base case, as it is shown in Figs. 3(c) and (d), and for this configuration the optimal value is located at $B/b = 4.0$, when $L/L_h = 3.0$. In this case, too, at $L/L_h = 1.5$, a poor improvement of the thermal performance is exhibited, whereas at $L/L_h = 3.0$ any B/b determines wall temperatures lower than those without a chimney.

The temperature profiles as a function of X, with $L_h/b = 2.5$ and $q_\Omega = 300$ and 450 W m^{-2} for $L/L_h = 1.5$ and 3.0 and several expansion ratio values, are reported in Fig. 4. The edge effects are more remarkable in this figure than in the case for $L_h/b = 5.0$ (Fig. 3). One can notice that the differences among the curves at different B/b values in Fig. 3 are smaller than those in Fig. 4. In

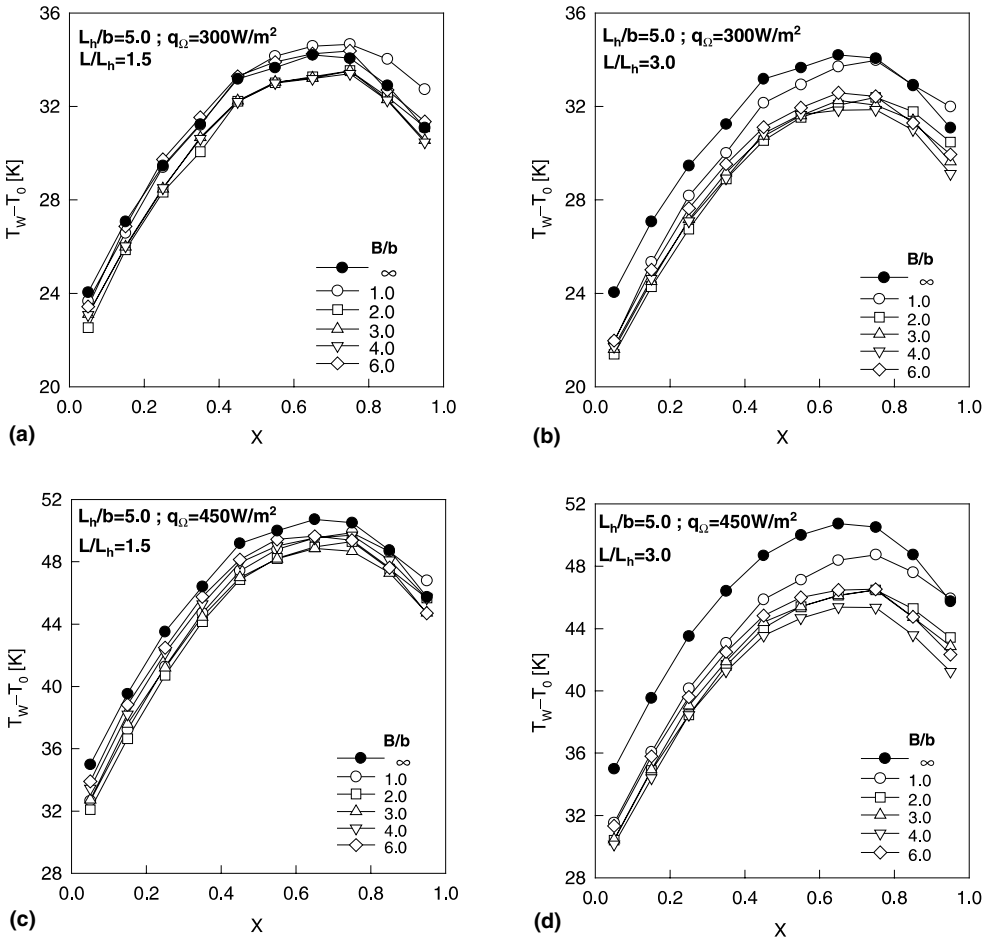

Fig. 3. Wall temperature profiles with $L_h/b = 5.0$ for several expansion and extension ratio values and two ohmic wall heat fluxes.

addition, wall temperatures are slightly larger at $L_h/b = 2.5$ than at $L/L_h = 5.0$, at the same B/b value. As it was previously observed, the fluid dynamic shroud behaves worse for the lower L/L_h values.

5.2. Maximum wall temperatures

What was previously observed is well summarized in Figs. 5–7, where the maximum wall temperatures as a function of the expansion ratio B/b and for several extension ratios, L/L_h, are shown. In Fig. 5 the profiles with an aspect ratio $L_h/b = 10$ and various heat flux values are reported. Fig. 5(a) ($q_\Omega = 50$ W m^{-2}) shows that when $B/b = 1.0$ and 8.0, the thermal performance is always worse than that of the base case ($L/L_h = 0$), whereas almost all other configurations perform better than the base case. At $L/L_h = 1.5$ an asymptotic behavior is attained at increasing B/b and, in addition, the optimal configuration is found at $B/b = 2.0$, for any L/L_h. Fig. 5(b) ($q_\Omega = 100$ W m^{-2}) shows that only for $B/b = 1.0$, some configurations show a greater ΔT_{max} than that in the base case. We can notice that the optimal value of B/b is equal to 2.0 for $L/L_h = 1.5$ and 2.0, while this value increases for $L/L_h = 3.0$. Besides, an asymptotic trend of the maximum wall temperatures is observed as B/b increases. This pattern can be easily explained since the more B/b increases, the more it gets closer to the limit value $B/b \to \infty$, i.e. the base case. On the contrary, Fig. 5(c) ($q_\Omega = 300$ W m^{-2}) clearly shows that the optimal configuration is always obtained at $B/b = 2.0$, whichever the L/L_h, and an asymptotic behavior is observed with B/b. The thermal performance of the channel is the worst for B/b greater or equal to 3.0 and $L/L_h = 1.5$.

The ΔT_{max} values at $L_h/b = 5.0$ are represented in Fig. 6. Fig. 6(a) ($q_\Omega = 100$ W m^{-2}) shows that at B/b smaller than 3.0, the configuration with $L/L_h = 2.0$ optimizes the thermal performance whereas at B/b larger than 3.0, the larger the L/L_h, the smaller the ΔT_{max}. Fig. 6(b) ($q_\Omega = 300$ W m^{-2}) exhibits increasing ΔT_{max} values at increasing L/L_h values. Comparing Fig. 5(c) to Fig. 6(b) shows that, as the channel aspect ratio (L_h/b)

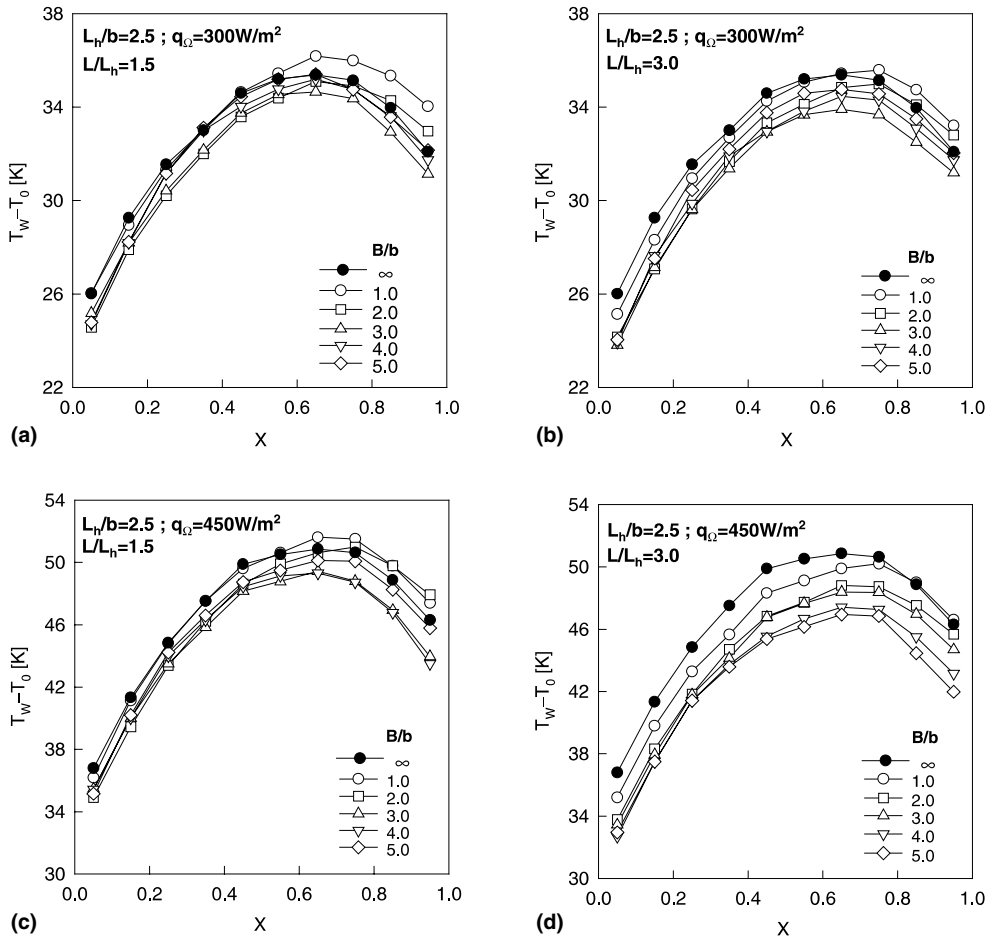

Fig. 4. Wall temperature profiles with $L_h/b = 2.5$ for several expansion and extension ratio values and two ohmic wall heat fluxes.

decreases, the optimal value of B/b shifts from 2.0 to 3.0 and in both cases ΔT_{max} decreases at increasing L/L_h. In Fig. 6(c) ($q_\Omega = 450$ W m^{-2}) the value of B/b which implies a minimum ΔT_{max} is equal to 3.0 when $L/L_h = 1.5$, while for larger L/L_h values the optimal expansion ratio is about 4.0. Anyway, it should be pointed out that the differences between the ΔT_{max} are not larger than 0.5°C when $B/b \geqslant 2.0$.

The same quantities as in Fig. 6, for $L_h/b = 2.5$ and at different q_Ω, are reported in Fig. 7. The optimal B/b values are greater, Fig. 7(a), than those for the corresponding configurations in Figs. 5 and 6. Furthermore, when $L/L_h \geqslant 3.0$ the optimal B/b values are larger than at lower L/L_h values. As q_Ω increases, the optimal value of B/b also increases and when $q_\Omega = 300$ W m^{-2} (Fig. 7(b)), it lies between 3.0 and 4.0 at L/L_h lower than 4.0, while for $L/L_h = 4.0$ the system is not affected by the B/b increase. When $q_\Omega = 450$ W m^{-2} (Fig. 7(c)), the configurations at $L/L_h = 1.5$ and 2.0 exhibit optimal values of B/b, whereas at $L/L_h \geqslant 3.0$ there is no B/b value which markedly optimizes the heat transfer. One can, therefore, conclude that an extension length nearly equal to the channel length ($L/L_h = 2.0$) and an expansion ratio (B/b) equal or larger than 2.0 determine a marked reduction in the maximum wall temperatures. Similarly, decreasing the channel aspect ratio (L_h/b) requires increasing B/b values in order to avoid the increase in maximum wall temperatures.

5.3. Correlations for dimensionless maximum wall temperatures and average Nusselt numbers

The dimensionless maximum wall temperatures, Eq. (6), as a function of the channel Rayleigh number times the expansion ratio, for the investigated L/L_h values, are reported in Fig. 8. Two monomial correlations between the $\Delta T_{max}, Ra^*(B/b)$ and L/L_h have been proposed for two different ranges of $Ra^*(B/b)$: 10^{-1}–10^2 and 10^2–5.0×10^6, namely

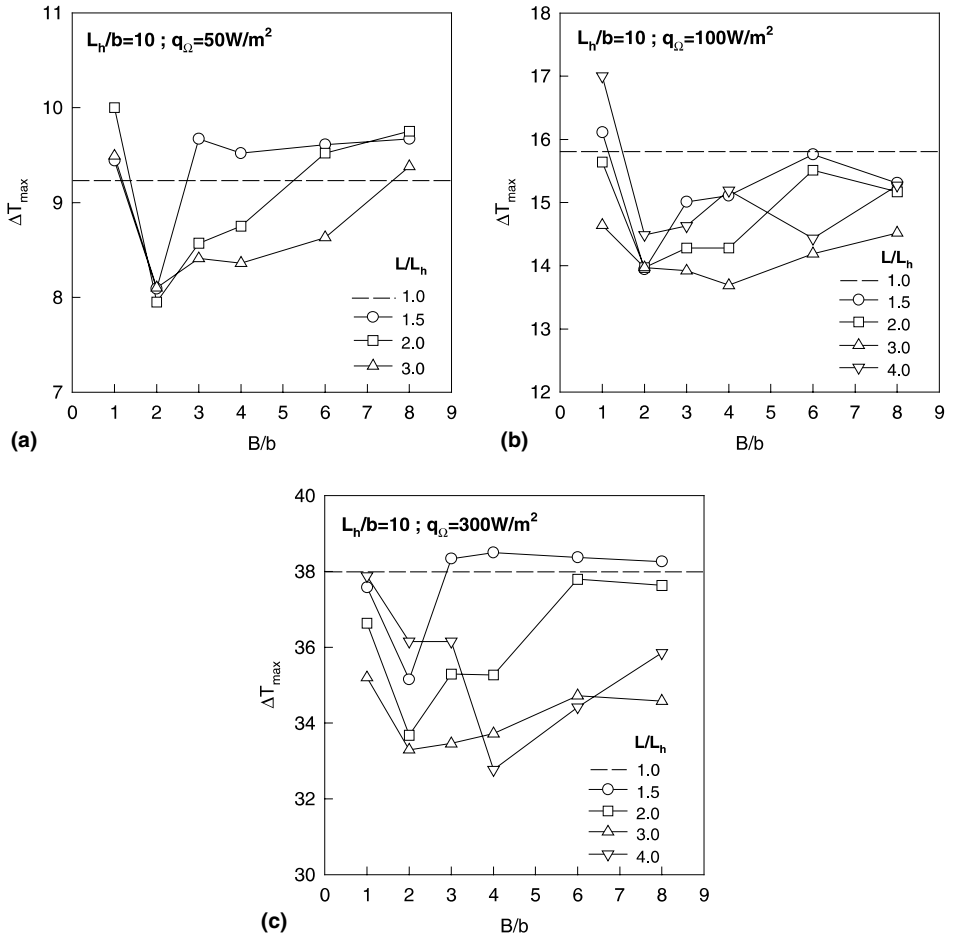

Fig. 5. Maximum wall temperatures as function of the expansion ratio B/b and several extension ratios with $L_h/b = 10$ for three ohmic heat flux values: (a) 50 W m^{-2}, (b) 100 W m^{-2}, and (c) 300 W m^{-2}.

$$\Delta T^*_{\max} = 7.32\left(Ra^*\frac{B}{b}\right)^{-0.416}\left(\frac{L}{L_h}\right)^{-0.0551} \tag{9}$$

with the regression coefficient $r^2 = 0.984$, in the $1.5 \leqslant L/L_h \leqslant 4.0$, $1.0 \leqslant B/b \leqslant 4.0$ and $10^{-1} \leqslant Ra^*B/b \leqslant 10^2$ ranges and

$$\Delta T^*_{\max} = 1.35\left(Ra^*\frac{B}{b}\right)^{-0.191}\left(\frac{L}{L_h}\right)^{-0.0317} \tag{10}$$

with $r^2 = 0.975$, in the $1.5 \leqslant L/L_h \leqslant 4.0$, $1.0 \leqslant B/b \leqslant 4.0$ and $10^2 \leqslant Ra^*B/b \leqslant 5.0 \times 10^6$ ranges.

The first correlation, Eq. (9), was obtained as the asymptotic limit to the fully developed flow ($Ra^* \to 0$). The second one, Eq. (10), represents the asymptotic limit to the single plate ($Ra^* \to \infty$). It should be observed that there is a very weak dependence of the $\Delta T_{\max}$ on L/L_h. By following the suggestions of [24], a composite correlation is now proposed for the full investigated range

$$\Delta T^*_{\max} = \left\{\left[1.35\left(Ra^*\frac{B}{b}\right)^{-0.191}\left(\frac{L}{L_h}\right)^{-0.0317}\right]^{1.74} + \left[7.32\left(Ra^*\frac{B}{b}\right)^{-0.416}\left(\frac{L}{L_h}\right)^{-0.0551}\right]^{1.74}\right\}^{1/1.74} \tag{11}$$

with $r^2 = 0.974$, for $1.5 \leqslant L/L_h \leqslant 4.0$, $1.0 \leqslant B/b \leqslant 4.0$ and $10^{-1} \leqslant Ra^*B/b \leqslant 5.0 \times 10^6$.

The channel average Nusselt numbers as a function of $Ra^*(B/b)$, as suggested by [13], are reported in Fig. 9, for several L/L_h values. In order to avoid overlaps at different L/L_h, the average Nusselt numbers were multiplied by a numerical coefficient. The correlations between Nu, $Ra^*(B/b)$ and L/L_h were sought in the form proposed in [24]:

$$Nu = \left(\frac{L}{L_h}\right)^m\left\{\left[c_1\left(Ra^*\frac{B}{b}\right)^n\right]^q + \left[c_2\left(Ra^*\frac{B}{b}\right)^p\right]^q\right\}^{1/q}. \tag{12}$$

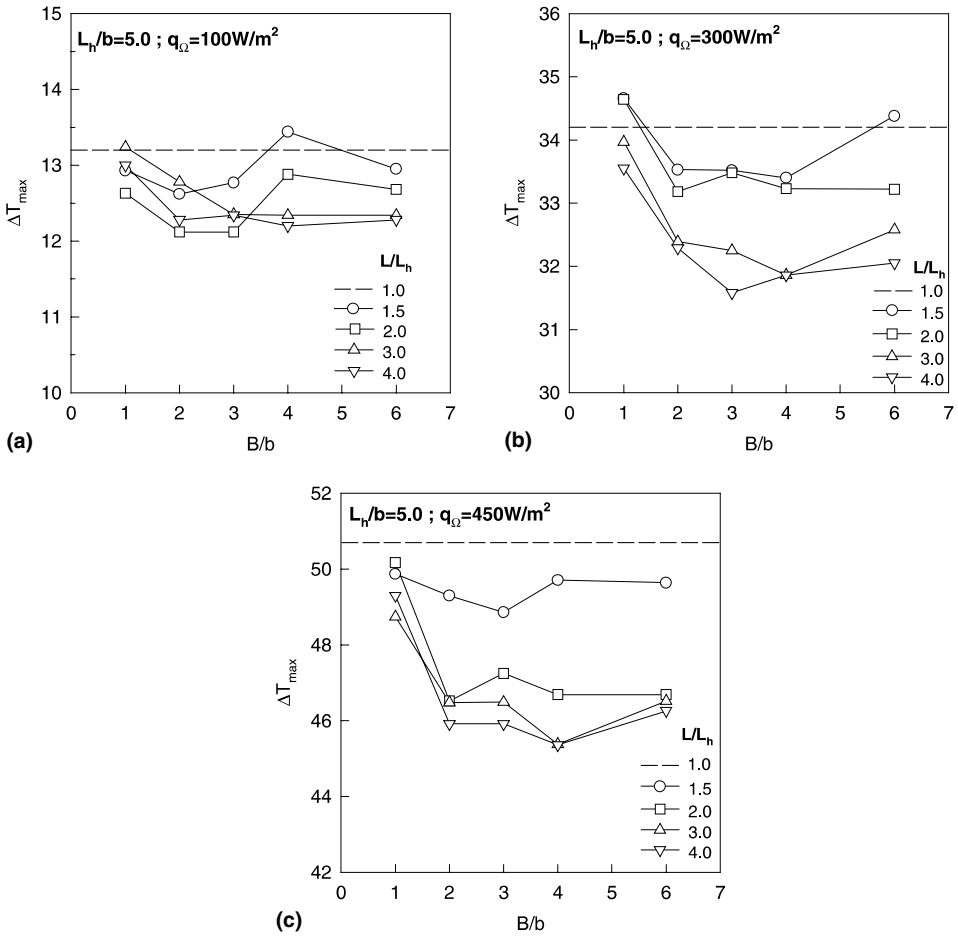

Fig. 6. Maximum wall temperatures as function of the expansion ratio B/b and several extension ratios with $L_h/b = 5.0$ for three ohmic heat flux values: (a) 100 W m^{-2}, (b) 300 W m^{-2}, and (c) 450 W m^{-2}.

When reference is made to the two asymptotic conditions, the fully developed flow proposed by [25] (with $c_1 = 0.288$ and $n = 0.500$) and the single plate limit, as suggested in [26] (with $c_2 = 0.730$ and $p = 0.200$) and the m and q parameters are obtained by means of a regression analysis, Eq. (12) reads

$$Nu = \left(\frac{L}{L_h}\right)^{0.100} \left\{ \left[0.288 \left(Ra^* \frac{B}{b} \right)^{0.500} \right]^{-1.32} + \left[0.73 \left(Ra^* \frac{B}{b} \right)^{0.200} \right]^{-1.32} \right\}^{-1/1.32} \quad (13)$$

with $r^2 = 0.965$, for $1.5 \leqslant L/L_h \leqslant 4.0$, $1.0 \leqslant B/b \leqslant 4.0$ and $10^{-1} \leqslant Ra^* B/b \leqslant 5.0 \times 10^6$.

When all the six parameters are obtained by means of the regression analysis, Eq. (12) is the following:

$$Nu = \left(\frac{L}{L_h}\right)^{0.0268} \left\{ \left[0.259 \left(Ra^* \frac{B}{b} \right)^{0.399} \right]^{-2.02} + \left[1.42 \left(Ra^* \frac{B}{b} \right)^{0.150} \right]^{-2.02} \right\}^{-1/2.02} \quad (14)$$

with $r^2 = 0.993$, for $1.5 \leqslant L/L_h \leqslant 4.0$, $1.0 \leqslant B/b \leqslant 4.0$ and $10^{-1} \leqslant Ra^* B/b \leqslant 5.0 \times 10^6$.

The above correlations are compared to the experimental results presented in Fig. 9 and a very good fit is found.

6. Conclusions

The temperatures measured in the experimental study on the chimney effect induced by adiabatic extensions downstream of two vertical parallel symmetrically he-

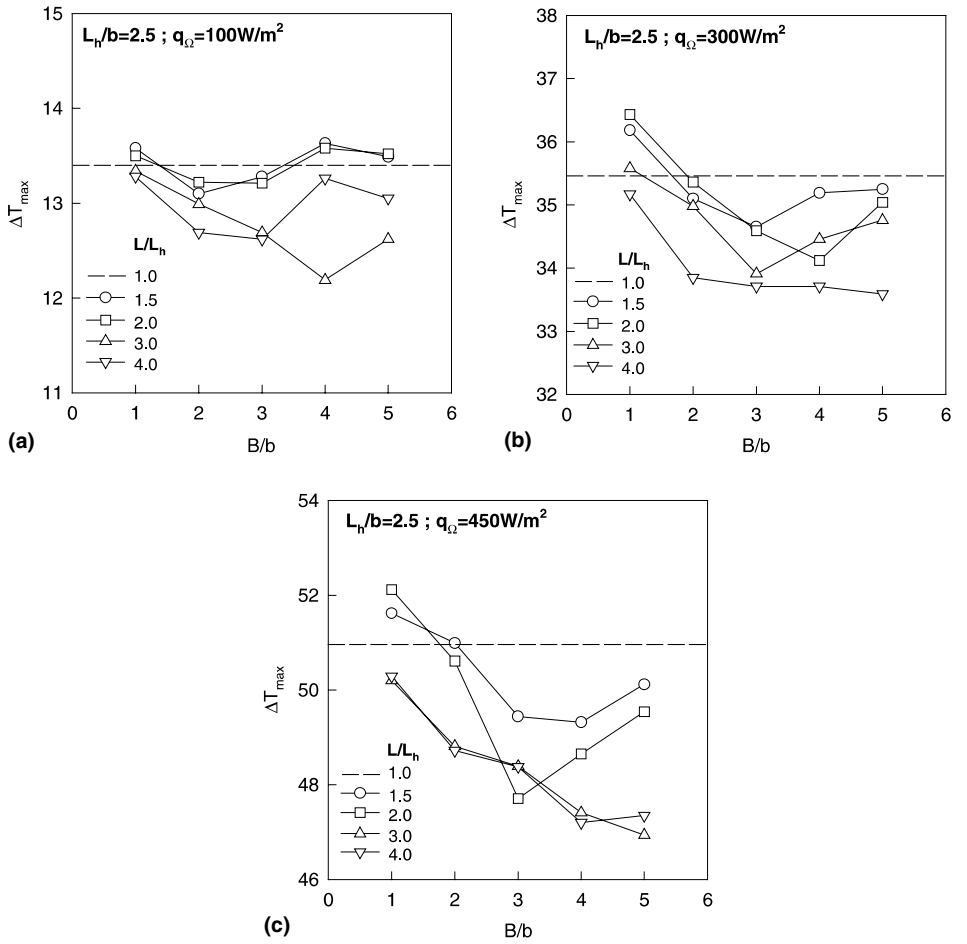

Fig. 7. Maximum wall temperatures as function of the expansion ratio B/b and several extension ratios with $L_h/b = 2.5$ for three ohmic heat flux values: (a) 100 W m^{-2}, (b) 300 W m^{-2}, and (c) 450 W m^{-2}.

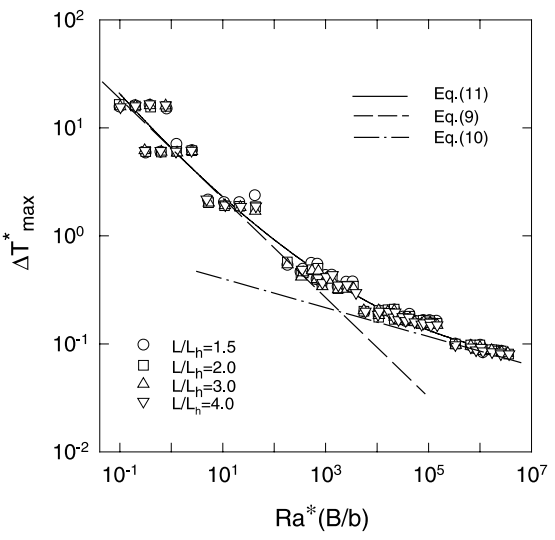

Fig. 8. Maximum wall temperature rise as function of the Ra^*B/b parameter for several extension ratios.

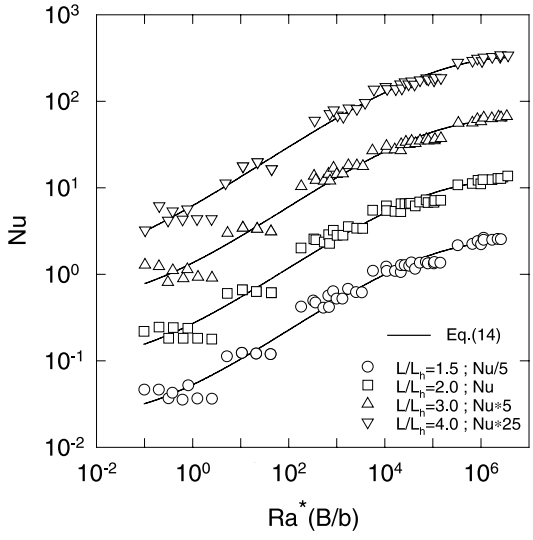

Fig. 9. Average Nusselt numbers as function of the Ra^*B/b parameter for several extension ratios.

ated isoflux walls show that in most investigated configurations the thermal performance is better than in the channel without the extensions (base case).

The experiments have been carried out for values of the extension ratio, i.e. the ratio of the total length, L, to the length of the heated region, L_h, in the 1.0 and 4.0 range and values of the expansion ratio, i.e. the ratio of the spacing of the adiabatic extension, B, and of the heated region, b, in the range 1.0–8.0. The channel Rayleigh number varied in the 10^{-1}–1.1×10^6 range. The experiments focused for Rayleigh number values greater than 1.8×10^2 and wall temperature profiles as a function of the extension and expansion ratios have been presented. Furthermore, the optimal channel configurations have been derived, which yield the minimum value of the maximum wall temperature. In most cases they are exhibited in the 2.0–3.0 range of the B/b ratio when L/L_h ratio is lower than 3.0 whereas the best thermal performance is exhibited for larger values of B/b when L/L_h is larger than 3.0. Finding an optimal configuration is in agreement with the predictions by Asako et al. [12] and is confirmed by the fact that when B/b tends to infinity, the channel configuration coincides with that in a channel without adiabatic extensions. The average channel Nusselt number in the channel with extensions increases in the 10–20% range when the channel Rayleigh number varies in the 1.8×10^2–1.1×10^6 range.

Finally, both dimensionless maximum wall temperatures and average channel Nusselt numbers have been correlated to the extension ratio, L/L_h, and to Ra^*B/b, in the $1.0 \leqslant L/L_h \leqslant 4.0$, $1.0 \leqslant B/b \leqslant 4.0$ and $1.0 \times 10^{-1} \leqslant Ra^*B/b \leqslant 5.0 \times 10^6$ ranges. All the correlations point out a weak effect of the extension ratio L/L_h on the thermal performance of the channel.

Acknowledgements

This research is supported by MURST under 1999 grant research program "Enhancement techniques in thermofluids".

References

[1] S.J. Kim, S.W. Lee, Air Cooling Technology for Electronic Equipment, CRC Press, Boca Raton, FL, 1996.
[2] G.A. Ledezma, A. Bejan, Optimal geometric arrangement of staggered vertical plates in natural convection, ASME J. Heat Transfer 119 (1997) 700–708 1997.
[3] D.A. Roberts, J.M. Floryan, Heat transfer enhancement in the entrance zone of a vertical channel, ASME J. Heat Transfer 120 (1998) 290–291.
[4] G.D. Raithby, K,G.T. Hollands, Natural convection, in: W.M. Rohsenow, J.P. Hartnett, Y.I. Cho (Eds.), Handbook of Heat Transfer Fundamentals, Chapter. 4, McGraw-Hill, New York, 1998.
[5] B. Gebhart, Y. Jaluria, R.L. Mahajan, B. Sammakia, Buoyancy Induced Flows and Transport, Hemisphere, Washington DC, 1988.
[6] G.P. Peterson and A. Ortega, Thermal control of electronic equipment and devices, in: T.F. Irvine, J.P. Hartnett (Eds.), Advances in Heat Transfer, vol. 20, Academic Press, New York, 1990, pp. 181–314.
[7] A. Campo, O. Manca, B. Morrone, Numerical analysis of partially heated vertical parallel plates in natural convective cooling, Numer. Heat Transfer – Part A 36 (1999) 129–151.
[8] B. Morrone, A. Campo, O. Manca, Optimum plate separation in a vertical parallel-plate channel for natural convection flows: incorporation of large spaces at the channel extremes, Int. J. Heat Mass Transfer 40 (1997) 993–1000.
[9] S.E. Haaland, E.M. Sparrow, Solutions for the channel plume and the parallel-walled chimney, Numer. Heat Transfer 6 (1983) 155–172.
[10] P.H. Oosthuizen, A numerical study of laminar free convective flow through a vertical open partially heated plane duct, ASME HTD 32 (1984) 41–48.
[11] R. A. Wirtz and T. Haag, Effects of an unheated entry on natural convection between heated vertical parallel plates, ASME Paper 85-WA/HT-14, 1985.
[12] Y. Asako, H. Nakamura, M. Faghri, Natural convection in a vertical heated tube attached to thermally insulated chimney of a different diameter, ASME J. Heat Transfer 112 (1990) 790–793.
[13] A.G. Straatman, J.D. Tarasuk, J.M. Floryan, Heat transfer enhancement from a vertical, isothermal channel generated by the chimney effect, ASME J. Heat Transfer 115 (1993) 395–402.
[14] K.T. Lee, Natural convection in vertical parallel plates with an unheated entry or unheated exit, Numer. Heat Transfer – Part A 25 (1994) 477–493.
[15] T.S. Fisher, K.E. Torrance, K.K. Sikka, Analysis and optimization of a natural draft heat sink system, IEEE Trans. on Components, Packaging Manufacturing Technol. – Part A 20 (1997) 111–119.
[16] T.S. Fisher, K.E. Torrance, Free convection limits for pin-fin cooling, ASME J. Heat Transfer 120 (1998) 633–640.
[17] N. Bianco, O. Manca, B. Morrone, V. Naso, Experimental analysis of chimney effect for vertical isoflux symmetrically heated parallel plates, in: Proceedings of the Eurotherm Seminar No. 58 on Thermal Management of Electronic Systems III, 1998, pp. 73–79.
[18] G.A. Shahin, J.M. Floryan, Heat transfer enhancement generated by the chimney effect in systems of vertical channel, ASME J. Heat Transfer 121 (1999) 230–232.
[19] T.S. Fisher, K.E. Torrance, Experiments on chimney-enhanced free convection, ASME J. Heat Transfer 121 (1999) 603–609.
[20] B.W. Webb, D.P. Hill, High Rayleigh number laminar natural convection in an asymmetrical heated vertical channel, ASME J. Heat Transfer 111 (1989) 649–656.
[21] S.J. Kline, F.A. McClintock, Describing uncertainty in single sample experiments, Mech. Eng. 75 (1953) 3–12.
[22] R.J. Moffat, Describing the uncertainties in experimental results, Exp. Thermal Fluid Sci. 1 (1988) 3–17.

[23] O. Manca, V. Naso, Experimental analysis of natural convection and thermal radiation in vertical channels, ASME HTD 145 (1990) 13–21.
[24] S.W. Churchill, R. Usagi, A general expression for the correlation of rates of transfer and other phenomenon, AIChE J. 18 (1972) 1121–1128.
[25] W. Aung, Fully developed laminar free convection between vertical parallel plates heated asymmetrically, Int. J. Heat Mass Transfer 15 (1972) 2293–2308.
[26] E.M. Sparrow, J.L. Gregg, Laminar free convection from a vertical plate with uniform surface heat flux, ASME J. Heat Transfer 76 (1956) 435–440.